Arab J Geosci (2016) 9: 732
DOI 10.1007/s12517-016-2755-5

ORIGINAL PAPER

Stable water isotopes of precipitation in China simulated by SWING2 models

Yanjun Che[1] · Mingjun Zhang[1] · Shengjie Wang[1] · Jie Wang[1] · Yangmin Liu[1] · Fuxian Zhang[1]

Received: 3 October 2015 / Accepted: 15 November 2016 / Published online: 25 November 2016

Abstract The stable water isotope ratio in precipitation is a useful tracer of atmospheric circulation. Such observations, however, are very limited in space and time. To solve this problem, many isotope-enabled general circulation models (GCMs) are used to help the interpretation of isotope proxies. In this paper, several isotope-enabled GCMs released by the second Stable Water Isotope Intercomparison Group (SWING2) were selected to assess the spatial pattern of deuterium (δD) and the deuterium excess (d) of precipitation in China. The isotopic data of the Global Network of Isotopes in Precipitation (GNIP) and the Chinese Network of Isotopes in Precipitation (CHNIP) were also applied to verify the simulations. The results indicate that these models accurately simulate the spatial characteristics of δD and d of precipitation in China. The correlation between the observations and simulations for LMDZ is the highest among these models, while the root-mean-square (RMS) and standard deviation are not perfect. In addition, LMDZ is worse than other models in capturing the low signal in certain regions, such as CAM, GISS_E, and MIROC. For the monthly variation, most SWING2 models underestimate δD of the precipitation but overestimate the value of d, except for isoGSM. The simulated monthly variation of the water isotopes from SWING2 models is in general similar to the observations, and the trend corresponds to the monthly variation in the Northern Hemisphere. Moreover, all models are good at illustrating the temperature and precipitation amount effects, while they exhibit varying skills in interpreting the altitude and continental effects.

✉ Mingjun Zhang
mjzhang2004@163.com

[1] College of Geography and Environmental Science, Northwest Normal University, Lanzhou, China

Keywords Isotopic composition · GCM · GNIP · China

Introduction

Stable water isotopes are widely used in studies of modern hydrological processes and paleoclimate reconstruction (Dansgaard 1964; Dincer 1968; Gat et al. 1969; Pfahl and Sodemann 2014; Worden et al. 2007). To understand the moisture source of the precipitation, the isotopic ratios of precipitation samples were measured. This work can be dated back to the mid-twentieth century. The Global Network of Isotopes in Precipitation (GNIP) was established in 1961 by the International Atomic Energy Agency (IAEA) and the World Meteorological Organization (WMO). More than 1000 stations have participated in this network until now. The GNIP database with a large number of monthly isotope data of precipitation has attracted considerable attention in hydrological studies, and there are more than 20 stations of China in this database (e.g., Li et al. 2014; Xi 2014; Wang et al. 2015). Based on the GNIP stations in China, Zhang et al. (2004) analyzed the seasonal variation of δ^{18}O of precipitation and the multiple moisture paths in China. Li et al. (2014) also studied the seasonal features of isotopes and deuterium excess (d) of the precipitation during summer and winter using GNIP stations in China and established a relationship between the stable water isotopes and air temperature. However, the remote region of western China (including the Tibetan Plateau and arid northwestern China) is not well-covered by GNIP and the GNIP observations in China stopped around 2000. In the 2000s, more precipitation networks on the regional or national scale were established in China. Tian et al. (2007) studied the spatial distribution of ^{2}H, ^{18}O, and d of precipitation in western China and assessed the impact of the Asian monsoon and westerlies on moisture. In addition, a new nationwide network called the

China Network of Isotopes in Precipitation (CHNIP) was set up, based on the Chinese Ecosystem Research Network (CERN), which provides more information about mechanisms of stable water isotopes of precipitation in China (Song et al. 2007; Liu et al. 2014).

Although there are several observation networks of isotopes of precipitation in China, as mentioned above, they are still limited for the interpretation of patterns in hydrological processes. Therefore, simulations of stable isotopes of precipitation and/or vapor are needed in China, especially for the desert and mountainous areas. In the past decades, the general circulation models (GCMs) in combination with water isotopes have been used to investigate the hydrological processes between the atmosphere and the Earth's surface. These isotope-equipped GCMs include complex physical processes such as radiation, advection, diffusion, convection, and other physical processes of isotopic fractionation. The GCMs provide new insights into the present and past climate and are considered effective methods in isotope hydrology (Xi 2014). The simulations of isotope-equipped GCMs not only restructure the tempo-spatial distribution of the isotopes ($H_2{}^{18}O$ and HDO) but also interpret the kinetic and thermal effects of the isotopic fraction of the hydrological cycle (Haese et al. 2013). Because of the multiple simulation methods conducted by different research groups, the simulation outputs of these models show significant differences and the intercomparison of GCM simulations is needed (AGU 1995; Sturm et al. 2010). To assess the simulations of the stable water isotopes, the Stable Water Isotope Intercomparison Group (SWING) was set up by international groups from multiple countries. The SWING simulations were applied in eastern Asia and showed a good agreement of the isotopic characteristics derived from long-term observations (Zhang et al. 2011, 2012).

The second phase of SWING (SWING2) has attracted more research groups to GCM simulations. These isotope-enabled GCMs were compared with the corresponding vapor isotope data derived from remote sensing (Risi et al. 2012a, 2012b), which indicated that the spatial distribution of δD in water vapor can be well simulated by those models, although certain discrepancies still exist. Conroy et al. (2013) assessed the simulation of the tropical Pacific Ocean from SWING2 models and found that the use of the single model for the interpretation of the regional paleoclimate should be treated with caution. However, further assessment of the SWING2 simulation in China is still scarce. The investigation of the multiple GCM-simulated isoscapes may provide useful information on the model selection for a specific region and period, as well as on hydrological processes without sufficient in-situ measurement in China. In this paper, we analyzed the basic pattern of the stable water isotope in China using isotope-equipped GCMs released by SWING2 with the aims of simulating the spatial pattern of the isotope of precipitation in China and assessing the performance of the SWING2 models in China.

Study method and data

Observation data of the stable water isotope

To verify the simulations from isotope-enabled GCMs, the observation data of isotopes of the precipitation in China were obtained from the GNIP and CHNIP databases. The GNIP data were published by IAEA/WMO on a monthly and annual basis and is available at http://www.iaea.org/water. The CHNIP only provides long-term annual mean data, which is acquired from Liu et al. (2014). To remove the influence of short-term observations of the GNIP database, we only selected the continuous stations with monthly data of no less than 20. Finally, a total of 30 sites from GNIP and 28 sites (the site of Erdos was removed due to mismatch of the coordinate information) from CHNIP (Fig. 1) were chosen.

Isotope-equipped GCMs

The simulation outputs of seven isotope-equipped GCMs (CAM, ECHAM, GISS_E, HadAM, isoGSM, LMDZ, and MIROC) were provided by SWING2 on the NASA–GISS website at http://www.giss.nasa.gov/projects/swing2. In this study, six models (CAM, ECHAM, GISS_E, isoGSM, LMDZ, and MIROC) were selected. It should be mentioned that the LMDZ model has two types of output, which are labeled LMDZ and LMDZfree in this study. The former is nudged by ECMWF and the latter is free. All simulations include the isotopic ratios of vapor and precipitation on a monthly basis, except for isoGSM and HadAM with vapor data only. More information on the simulations from the SWING2 models is listed in Table 1.

Methods

The stable isotopic composition of the precipitation and vapor is expressed as a deviation from the standard mean ocean water (SMOW) in per million (‰):

$$\delta(‰) = \left[\frac{R}{R_{\mathrm{SMOW}}} - 1\right] \times 1000,$$

where R = oxygen-18/oxygen-16 is the concentration ratio between the heavier isotope and the common water molecule. The deuterium excess ($d = \delta\mathrm{D} - 8\delta^{18}\mathrm{O}$; Dansgaard 1964), a two-order isotopic parameter linking δD and δ^{18}O, is also calculated in this study. Besides, when reading the output data derived from those isotopic models, the rarely anomalous data are found and removed in the calculating process.

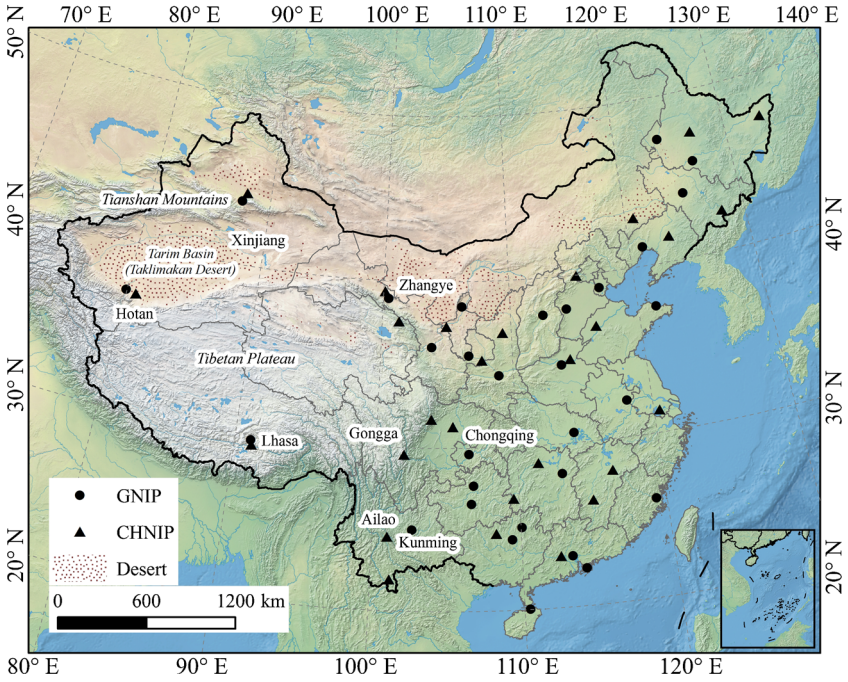

Fig. 1 Spatial distribution of GNIP and CHNIP sites in China selected in this study

Spatial pattern and monthly variation of δD in precipitation

Spatial pattern of δD of precipitation

The spatial pattern of δD of the precipitation is jointly controlled by geographical and meteorological factors. The regime is usually known as, for instance, latitudinal effect, continental effect, altitude effect, and amount effect (Araguás-Araguás et al. 2000). As shown in Fig. 2a, b, the value of δD is relatively positive on China's southeast coasts but negative in the northwest and northeast portions and the Tibetan Plateau. The spatial characteristics in this study generally correspond to the summary of "three high-value regions and four low-value regions" in China by Gu (2011).

The isotope-equipped GCMs (Fig. 2c–h) provide the isoscapes of the precipitation with spatial continuity, which is meaningful for the regions without enough in situ observations, especially in western China. The simulated spatial distributions are generally similar to that of the GNIP and CHNIP databases, with a decreasing trend in δD from the southeast coast to the northwest inland. However, there are still some discrepancies between the simulations and observations. It is clear that the magnitudes of δD of the precipitation simulated by the SWING2 models are different from that of the GNIP and CHNIP databases to some degree. Figure 2c, e, h shows that the simulated minimum of δD (CAM, GISS_E, and MIROC) is significantly lower than that of the observations (Fig. 2a, c). The scarce network at the high elevation of the Tibetan Plateau may be the main reason for this difference. Figure 1 indicates that there is only one station (Lhasa) on the Tibetan Plateau, which leads to a poor spatial representation for such a large plateau. The potential low-value region of the Tibetan Plateau is simulated by several GCMs, although the magnitudes vary for each model. In

Table 1 Primary information on isotope-equipped GCMs in this study

GCM	Horizontal resolution (longitude × latitude)	Vertical resolution	Period	Simulation type	Typical references
CAM	128 × 64	26	1958–2007	Free	Lee et al. (2007)
ECHAM	128 × 64	19	1956–2001	Nudged with ECMWF	Hoffmann et al. (1998)
GISS_E	72 × 46	20	1965–2004	Nudged with NCEP	Schmidt et al. (2007)
HadAM	96 × 73	17	1958–2003	Free	Tindall et al. (2009)
isoGSM	144 × 73	17	1979–2007	Nudged with NCEP	Yoshimura et al. (2008)
LMDZ	96 × 72	19	1979–2007	Free and nudged with ECMWF	Risi et al. (2010)
MIROC	128 × 64	20	1979–2007	Free	Kurita et al. (2011)

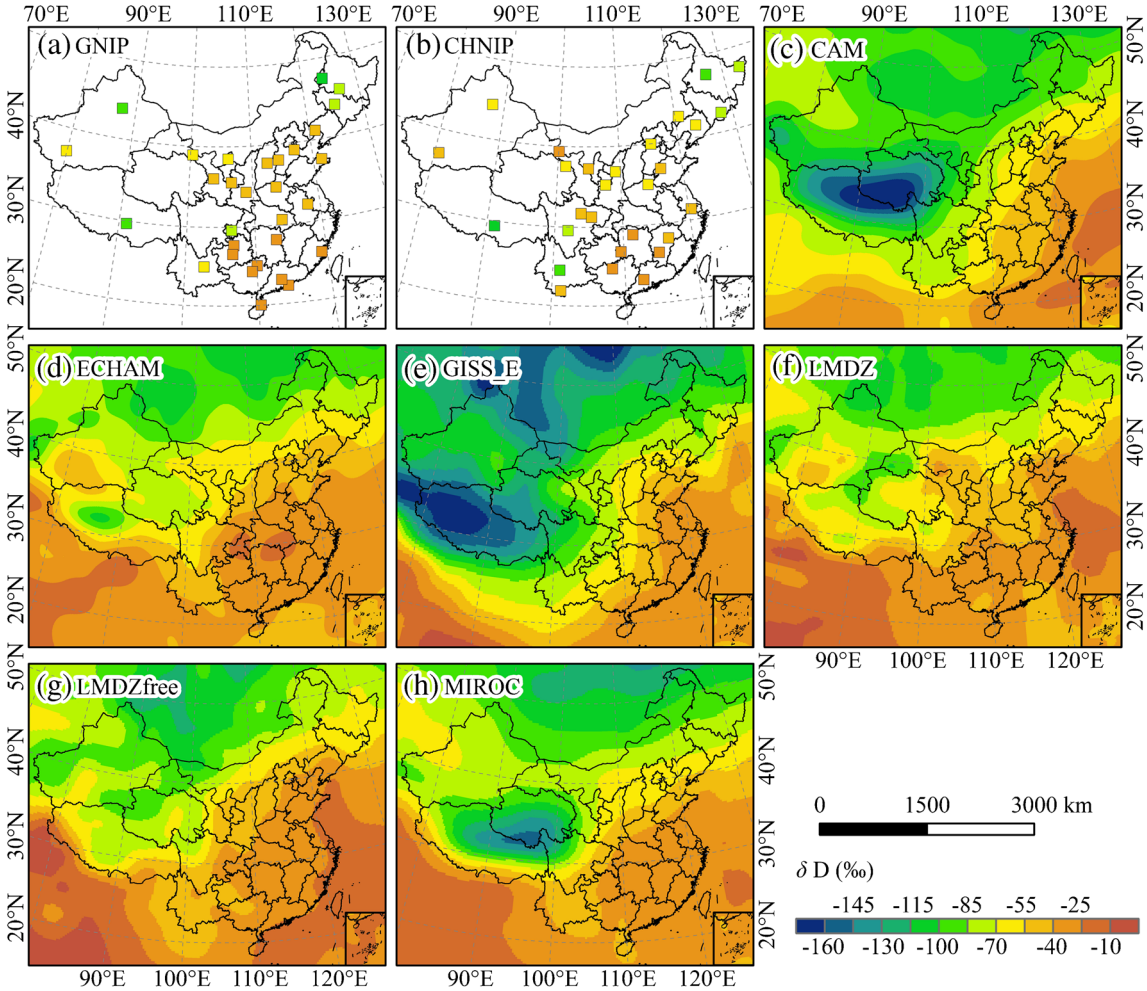

Fig. 2 Spatial distribution of the annual mean δD of the precipitation in China derived from the GNIP and CHNIP databases and isotope-enabled GCMs. In plots, **a** and **b** are eExpressive of the δD of precipitation from GNIP and CHNIP databases observed in China, respectively. Plots **c**–**h** are expressive of the δD of precipitation in China derived from models, in order, corresponding to CAM, ECHAM, GISS_E, LMDZ, LMDZfree, and MIROC

addition, GCM-modeled high-value regions of δD usually occur in the southeastern coastal region, southern tropical regions, and southern Xinjiang (Tarim Basin). Relatively low values of δD are observed in the northeast region, northern Xinjiang, and the Tibetan Plateau. Although the precipitation-δD modeled by ECHAM, LMDZ, and LMDZfree (Fig. 2d, f, g) is lower than that modeled by CAM, GISS_E, and MIROC (Fig. 2c, e, h), it seems that it has a similar magnitude to that of GNIP and CHNIP.

It is difficult to assess these models directly for the simulation of isotopes of the precipitation for such a large region. However, the Taylor diagram assesses multiple models, which can provide a method of graphically summarizing how closely a pattern (or a series of patterns) matches the reference model or observational data (Taylor 2001). To assess the simulation quality of SWING2 models in China, statistical indexes were calculated including the correlation coefficient (CC), standard deviation (SD), and centered root-mean-square (RMS) difference (Fig. 3). The GNIP data were taken as reference (Fig. 3a). These simulations present the correlations between the observation (GNIP) and simulated δD well, which range from ~0.65 to ~0.8. Although most models (except CAM) show pattern correlation coefficients ≥0.7, there are large differences among the models. The standard deviation of the SWING2 models is either too low or too high compared to GNIP and hence relatively dispersed. For instance, in spite of the correlation coefficients of GISS_E and LMDZ (0.79 and 0.78, respectively), the GISS_E has a relatively high standard deviation (SD = 28.93‰), while the LMDZ has a very low standard deviation (SD = 13.25‰). The SWING2 models show similar RMS values, ranging from 12.77 to 18.45‰. Furthermore, we also considered CHNIP as reference to estimate the performance of the SWING2 models (Fig. 3b). It is indicated that the correlation coefficients of the models are relatively low, ranging from ~0.2 to ~0.6. The standard deviation in Fig. 3b is similar to that in Fig. 3a, ranging from ~10 to ~30‰. However, the RMS of the SWING2 models varies from 17.80 to 31.55‰. In general, the LMDZ are perfectly suitable to simulate the δD of precipitation

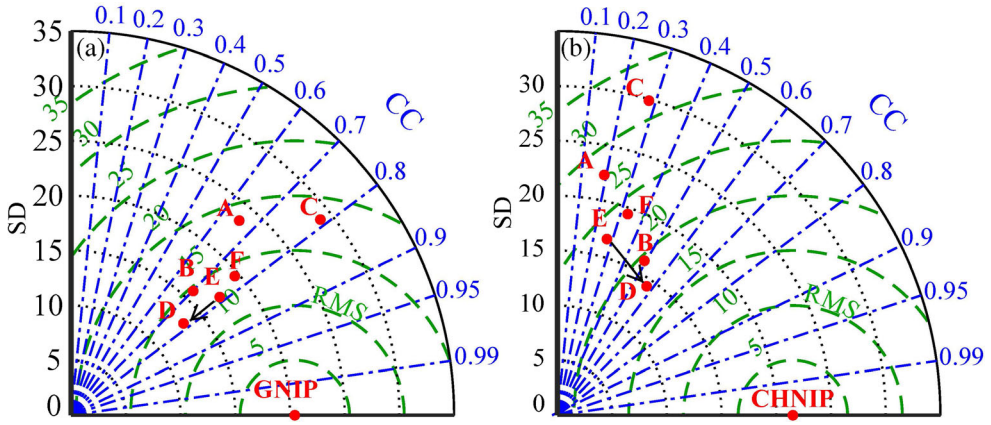

Fig. 3 Diagram displaying the pattern statistics. **a** The precipitation-δD in GNIP was used as reference data. **b** The precipitation-δD in CHNIP was used as reference data. The *capital letters A* to *F* in the plots correspond to the isotopic models in the order of CAM, ECHAM, GISS_E, LMDZ, LMDZfree, and MIROC. The radial distance in the diagrams from the origin is proportional to the standard deviation (SD) of a pattern (*black line*). The centered root mean square (RMS) difference between the model and reference field is proportional to their distance (*green line*). The correlation coefficient between the two fields is given by the azimuthal position of the model field. Moreover, the *black arrows* indicate the change from the "free" model simulation to the model nudged with reanalysis winds

in terms of CC and RMS. The MIROC of the standard deviations are closer to that of the observations. Moreover, the nudged LMDZ is significantly better than the free LMDZ in terms of simulated δD of precipitation and the correlation coefficient of the nudged LMDZ is ~0.6, which is larger than that of the free LMDZ (CC < 0.3; Fig. 3b).

To estimate the spatial variation of the modeled data, the mean value of δD of the precipitation in the meridional and latitudinal directions is calculated, respectively (Fig. 4). The value of δD of the precipitation of the meridional gradient decreases with increasing latitude (Fig. 4a, b), so do the GCM simulations (Fig. 4c) in China. This spatial pattern is defined as latitudinal effect (Gu 2011). However, there are three samples that deviate much more from the other samples in Fig. 4a, b. The three deviating points of GNIP in Fig. 4a are Kunming, Chongqing, and Lhasa. The three stations of CHNIP in Fig. 4b are Ailaoshan (Mts. Ailao), Gonggashan (Mts. Gongga), and Lhasa. The values of those sites are relatively more negative than the others at similar latitudes because they are in and around the Tibetan Plateau with high elevation and low air temperature. However, the influence of the plateau is only captured by CAM, GISS_E, and MIROC in all of the simulated data (Fig. 4c). The spatial pattern of the latitudinal gradient from the observations and simulations exhibits a similar variation (Fig. 4d–f), except for GISS_E west of 90°E, which shows adverse fluctuation compared with other models.

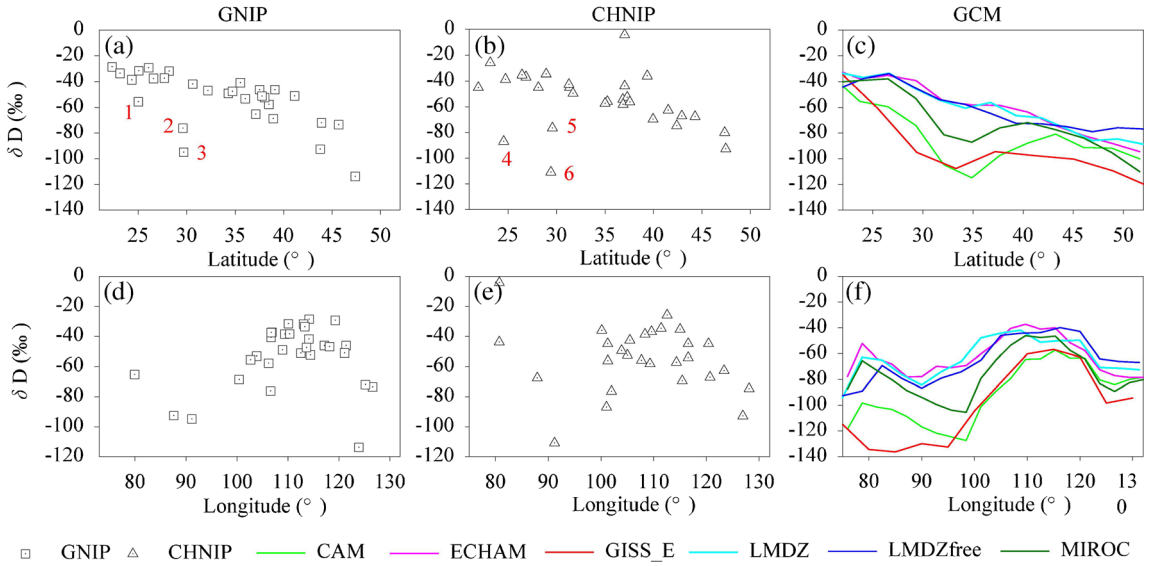

Fig. 4 Relationship between the latitude/longitude and δD of the precipitation in China derived from the GNIP and CHNIP databases and isotope-enabled GCMs. Typical stations are labeled with numbers, **a** *1* Kunming, *2* Chongqing, and *3* Lhasa; **b** *4* Ailaoshan, *5* Gonggashan, and *6* Lhasa

Spatial pattern of *d* of the precipitation

The spatial pattern of the precipitation-*d* in China is shown in Fig. 5a, b. There are great differences among the simulations from the SWING2 models (Fig. 5c–g). The value of *d* in the Tibetan Plateau region is relatively high, which can be observed in each model. Most simulations of the SWING2 models show that *d* is higher in the southeastern region than in the northern region of eastern China, except for Fig. 5h. The spatial distribution of *d* is largely controlled by the meteorological conditions of the vapor source region, such as the sea surface temperature, wind speed, relative humidity, and additional air masses mixed in the moving process.

The spatial trend of the meridional gradient is not very notable in the observational data of Fig. 6a, b. The same pattern is shown in Fig. 6c, which is simulated from GCMs. Discrepancies of the *d* variation are also irregular in the meridional direction. However, the curves of the simulation of the latitudinal gradient show a good consistency, which decreases from west to east (Fig. 6f) in China. This finding is another indication that the high value of *d* is in the western and the low value of *d* is in the eastern part of China, which is also described in Gu (2011). There are still some shortcomings when comparing simulations and observations and the distribution of the observation sites is not even in the latitudinal direction. Furthermore, it can be noted that the discrepancies in the western region at 105°E are larger than that in the eastern region at 105°E. The possible reason is that there are significantly less observation sites in western China than in eastern China.

Monthly variations of δD and *d* of the precipitation

The simulation performance of the SWING2 models was assessed on a monthly scale. Figure 7a shows that the simulated fluctuations of δD of the precipitation are consistent with the monthly variation of GNIP, except for isoGSM. However, the magnitudes of δD are different in these models, while the discrepancies are generally within 80‰. Compared to the GNIP data, these results show that the simulations lead to

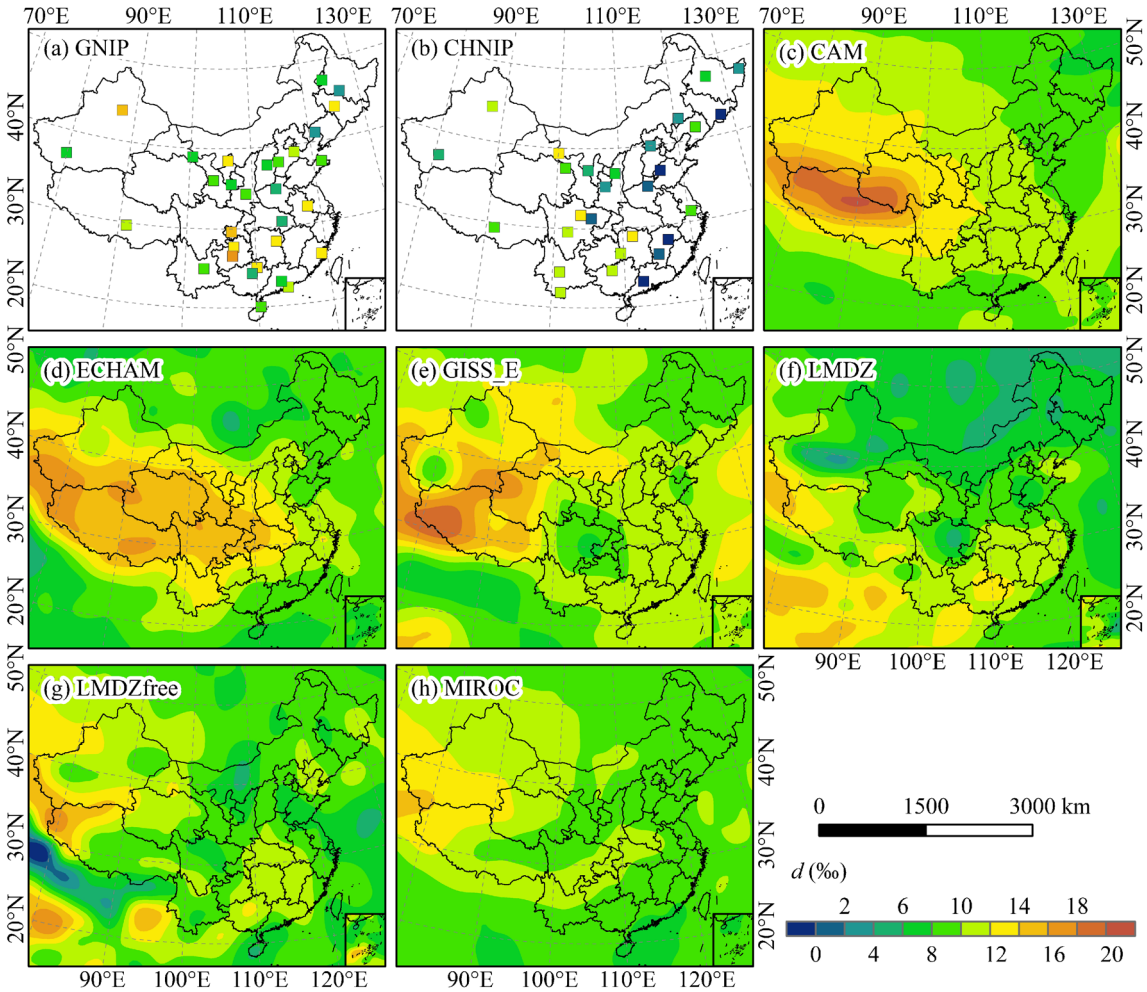

Fig. 5 Spatial distribution of the annual mean *d* of the precipitation in China derived from the GNIP and CHNIP databases and isotope-enabled GCMs

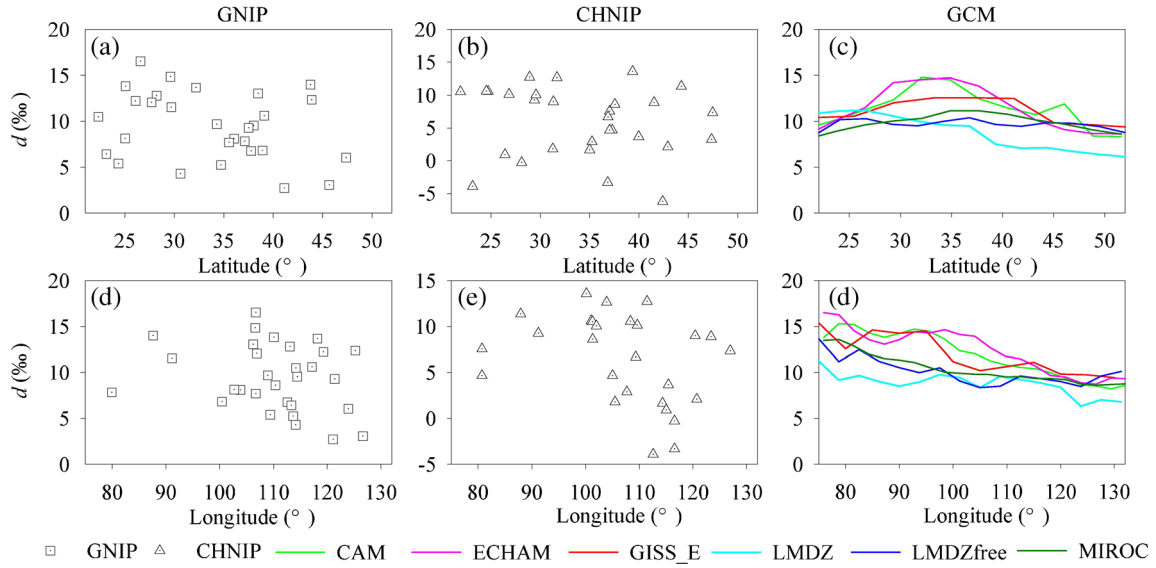

Fig. 6 Relationship between the latitude/longitude and *d* of the precipitation in China derived from the GNIP and CHNIP databases and isotope-enabled GCMs

underestimations on the monthly scale. In addition, the variation of δD modeled by isoGSM has an adverse trend from May to October with the GNIP data trend. The curves simulated by ECHAM, LMDZ, and LMDZfree show a good consistency with the curve of GNIP, while other models (CAM, GISS_E, and MIROC) show relatively larger fluctuation. The GNIP in China shows a relatively low value of *d* in the summer and a high value of *d* in the winter (Fig. 7b). This feature corresponds with the pattern of the Northern Hemisphere described by Schotterer et al. (1996), which could also be supported by the simulations from the SWING2 models. However, there are many discrepancies in the simulated results and most SWING2 models seem to overestimate the monthly precipitation. In addition, the simulated value of isoGSM is higher than that of the other models (CAM, ECHAM, GISS_E, LMDZ, LMDZfree, and MIROC). In spite of this, it is clear that the modeled curves of LMDZfree and MIROC are relatively closer to the curve of GNIP for monthly δD.

Factors influencing the pattern of precipitation-δD in China revealed by models

Altitude and continental effects on precipitation-δD

To understand the altitude and continental effects of the stable isotopes of the precipitation in China, the linear equations between precipitation-δD and ground elevation and the equations between precipitation-δD and continent were regressed. The regression equations indicate that δD of the precipitation decreases with increasing elevation (Table 2). In addition, the fitting optimization indexes of CAM and GISS_E are R^2 of 0.54 and 0.48, respectively. It can be noted that the results derived from CAM and ECHAM are better than that of other isotope models with respect to R^2 and larger than that of the observed GNIP ($R^2 = 0.15$, $p = 0.03$) and CHNIP ($R^2 = 0.15$, $p = 0.04$). Based on the output data from CAM and GISS_E, the linear gradients between the precipitation δD and the altitude are both of −1‰/

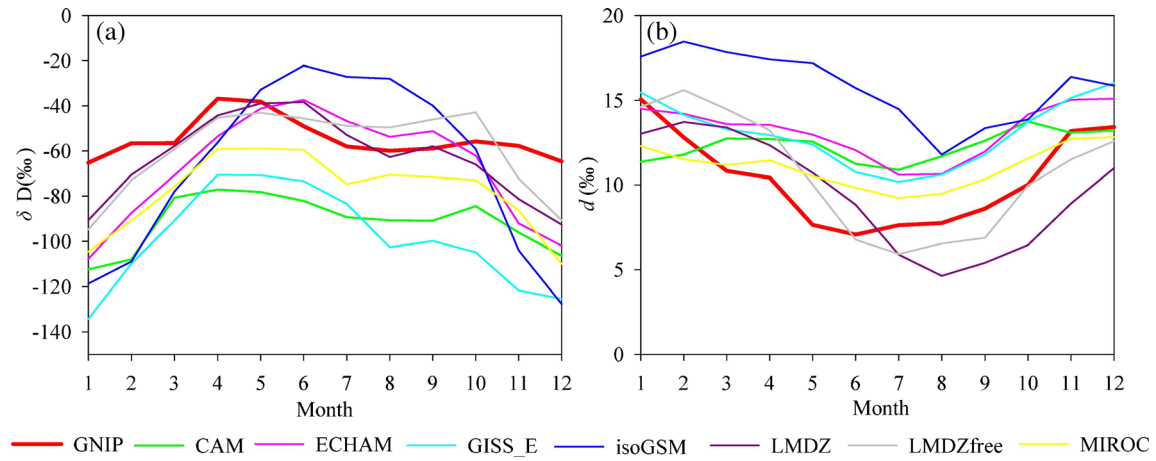

Fig. 7 Monthly variation of δD (**a**) and *d* (**b**) of the precipitation in China derived from the GNIP database and isotope-enabled GCMs

Table 2 Relation between δD and the elevation in GNIP, CHNIP, and isotope models, including CAM, ECHAM, GISS_E, LMDZ, LMDZfree, and MIROC

	Equation ($\delta D = k*H + b$)	R^2	*P* value
GNIP	$\delta D = -0.01*H - 47.57$	0.15	0.03
CHNIP	$\delta D = -0.01*H - 48.33$	0.15	0.04
CAM	$\delta D = -0.01*H - 65.41$	0.54	<0.001
ECHAM	$\delta D = -0.003*H - 54.58$	0.05	0.01
GISS_E	$\delta D = -0.01*H - 70.58$	0.48	<0.001
LMDZ	$\delta D = -0.004*H - 53.02$	0.12	<0.001
LMDZfree	$\delta D = -0.006*H - 50.34$	0.22	<0.001
MIROC	$\delta D = -0.01*H - 57.73$	0.28	<0.001

The parameter H is the ground elevation in meter

100 m in China and the GNIP sites in China show a similar gradient value of −1‰/100 m. Therefore, the models of CAM and GISS_E perform well in simulating the altitude effect of precipitation-δD in China.

To understand the continental effect of precipitation-δD in China, the linear equations between δD and the distances from the Pacific Ocean for different models are calculated and the equations are shown in Table 3. Based on the regression equation of different datasets, it can be noted that the δD of the precipitation decreases with increasing distance from the coastline to the inland. The linear gradients between the precipitation-δD of GISS_E and LMDZfree and the distance are −0.03‰/km ($R^2 = 0.64$, $p < 0.001$) and −0.02‰/km ($R^2 = 0.56$, $p < 0.001$) in China, respectively. Notably, the models' performance is better than that of the observed data from GNIP and CHNIP in interpreting the continental effect of precipitation-δD, with R^2 of 0.31 ($p = 0.001$) and 0.12 ($p = 0.07$), respectively. Hence, this finding indicates that the models of GISS_E and LMDZfree are suitable to reveal the continental effect of precipitation-δD in China.

Table 3 Relation between δD and the distance from the Pacific Ocean of the GNIP, CHNIP, and isotope models, including CAM, ECHAM, GISS_E, LMDZ, LMDZfree, and MIROC

	Equation($\delta D = k*D + b$)	R^2	*P*
GNIP	$\delta D = -0.02*D - 42.40$	0.31	0.001
CHNIP	$\delta D = -0.01*D - 48.36$	0.12	0.07
CAM	$\delta D = -0.02*D - 62.01$	0.40	< 0.001
ECHAM	$\delta D = -0.01*D - 45.67$	0.23	< 0.001
GISS_E	$\delta D = -0.03*D - 56.23$	0.64	< 0.001
LMDZ	$\delta D = -0.01*D - 43.90$	0.34	< 0.001
LMDZfree	$\delta D = -0.02*D - 38.50$	0.56	< 0.001
MIROC	$\delta D = -0.01*D - 54.29$	0.24	< 0.001

Note that the anomalous data (Cele site) of Liu et al. (2014) was removed in the regressing equation between δD and the distance from the ocean for CHNIP. The parameter *D* of the equations is the distance from the Pacific Ocean in km

The temperature and amount effects on precipitation-δD

The temperature and precipitation amount are major meteorological factors controlling the stable isotopes of precipitation. To assess the correlation between δD and the two meteorological factors in China, the correlation coefficient (CC) was calculated in this paper. Based on the observed data from GNIP, it is clear that the highly positive correlation between δD and the temperature mainly appears in the northwestern and northeastern part of China, with CC >0.8 (Fig. 8a). However, there is a negative correlation in the southern portion of China due to larger precipitation (Gu 2011). The results derived from the six models show the strong temperature effect in the northwestern and northeastern part of China (Fig. 8b–g), except for some transition regions such as Tibetan Plateau and the middle portion. In addition, the spatial patterns of the temperature effect of the models are notably better than those in the observation.

Based on the observed data in GNIP (Fig. 9a), the high negative correlation primarily occurs in the southern portion of China and is controlled by the precipitation amount as described in Gu (2011) and Zhang and Wang (2016). The CCof the southern portion of China is smaller than −0.6, which indicates that strong precipitation occurs in those regions with respect to δD of the precipitation (Fig. 9b–g). However, certain regions show different control effects in the models (Fig. 9). For instance, the northwestern portion and the Tibetan Plateau also have a larger precipitation amount effect due to the influence of the westerlies and the India monsoon, respectively (Zhang et al. 2004; Zhang and Wang 2016; Cai and Tian 2016). Therefore, the southern regions of China are governed by strong precipitation amounts, based on the observed data in GNIP and the output data from isotope models.

Discussion

The gradient of the isotopes of the precipitation in the longitudinal and latitudinal directions has been analyzed in previous studies. The patterns are sometimes summarized as continental effect, latitude effect, and so forth. The meridional gradient of δD of the precipitation decreases with the increasing latitude in Siberia, which was described in Gryazin et al. (2014) using SWING2 models. The SWING2 models overestimated the seasonal variation compared with the observational δD and underestimated the meridional gradient in the summer. However, in terms of the monthly variation of δD, our results show that the SWING2 models do not have a consistent behavior in depicting δD. Most of the

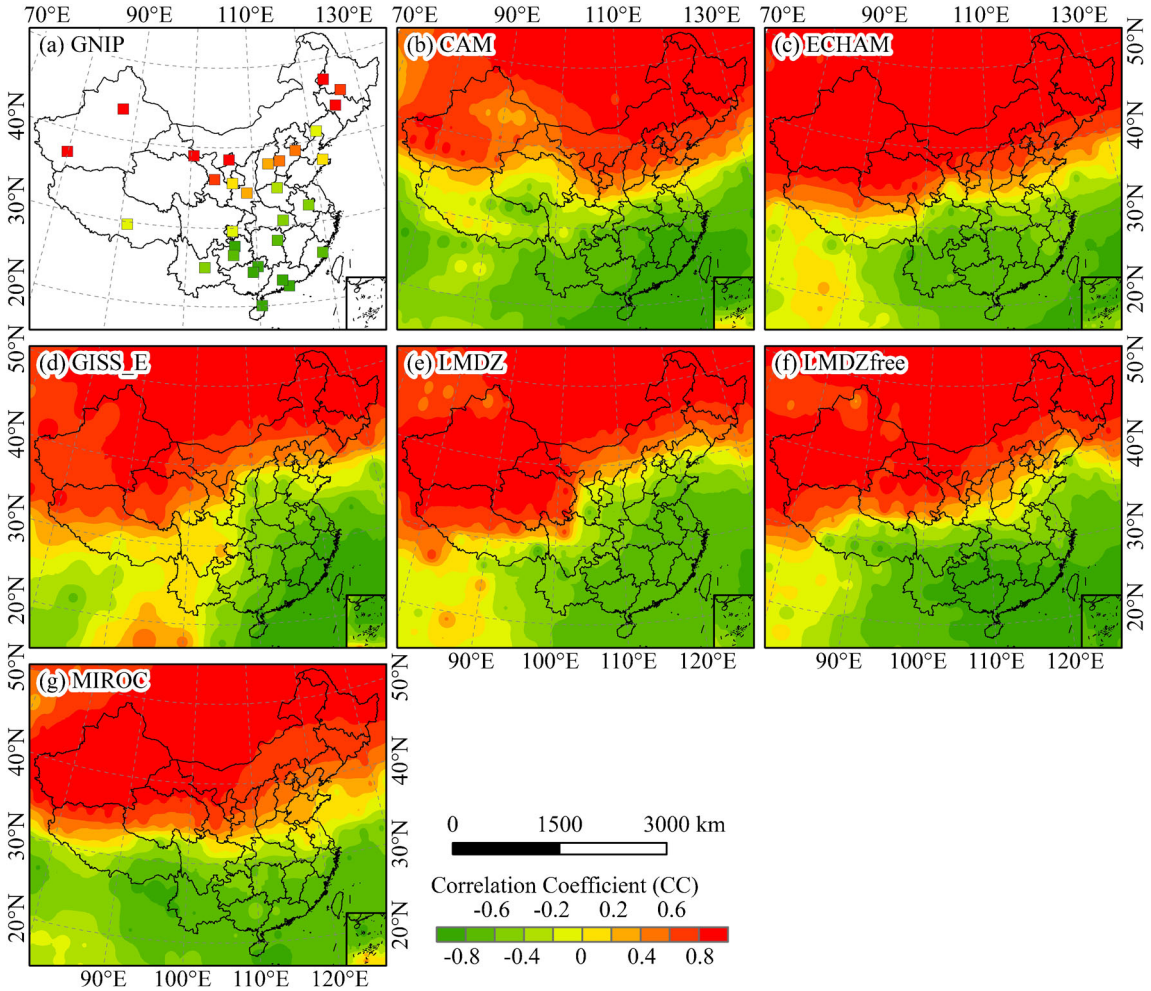

Fig. 8 The correlation coefficient (CC) between observation and models in spatial pattern of precipitation-δD in China. The temperature data in **a** are derived from http://www.iaea.org/water. The temperature data in **b**–**g** are derived from the output data of the models corresponding to precipitation-δD

SWING2 models (CAM, GISS_E, MIROC, and LMDZ) underestimate δD, but overestimation occurs during the warm season (from May to September) in other models (ECHAM, isoGSM, and LMDZfree). On the contrary, the decreasing trend in the meridional direction found in this work is the same as that of the study by Gryazin et al. (2014). Based on SWING, Zhang et al. (2011, 2012) studied the annual δD and *d* of precipitation in East Asia. They proved that there was a low-value region of δD (below −160‰) in the Tibetan Plateau. Likewise, this low value in the Tibetan Plateau was also found in the SWING2 models, but the magnitude of the low value is slightly different between the SWING and SWING2 models. Note that the region of low value simulated by ECHAM4 of SWING was not significant in the Tibetan Plateau, while it is very significant in the ECHAM4 of the SWING2 model.

The spatial pattern of precipitation-*d* shows the significant latitude effect modeled by the SWING models (ECHAM4, GISS_E, and MUGCM). There is a high-value region of precipitation-*d* in the Tibetan Plateau, which was also simulated by the SWING2 models in this paper. In addition, *d* of the precipitation increases from east to west in China because the water vapor originating from the ocean is the fundamental source of terrestrial precipitation. The isotopic fractionation incessantly takes place during the process of the vapor transportation toward the inland and polar regions. In the process of forming rain, the heavy isotope is previously condensed, leading to isotopic depletion. Likewise, raindrops evaporate in dry air at high temperatures. On the contrary, the heavy isotope often slowly vaporizes during evaporation. In addition, the fractionation velocity of the isotope composition is different, even under the same condition. As described by Gu (2011), *d* of the precipitation in western China is higher than that in eastern China and southern China usually has a higher value of *d* than the northern part of eastern China.

Based on the observations and remote sensing data, the simulated δD values of the SWING2 models were assessed on a global scale by Risi et al. (2012a, 2012b). These researchers found that these models could simulate the spatial pattern of the isotope (δD) of precipitation and the value of δD in summer

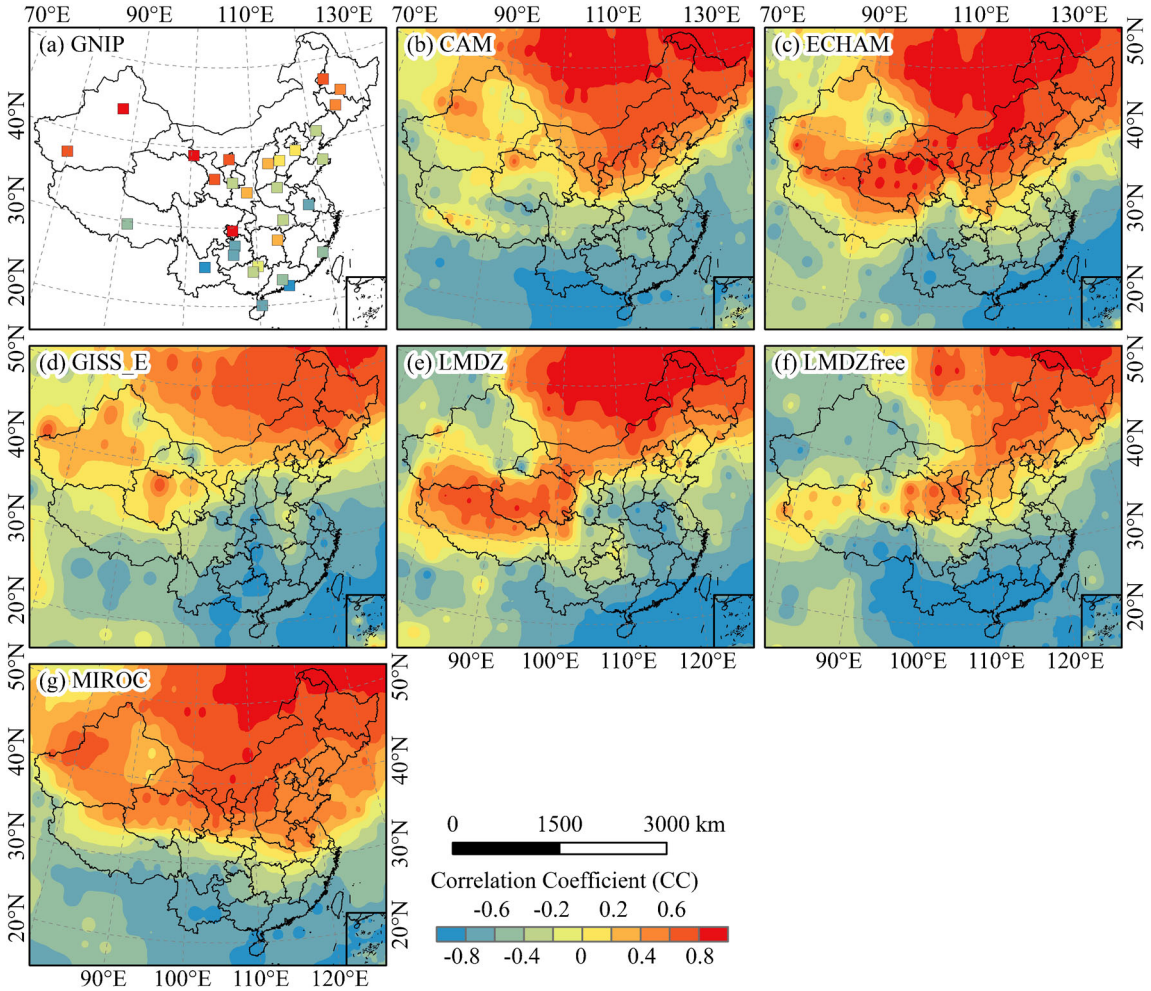

Fig. 9 The correlation coefficient (CC) between observation and models in spatial patterns of precipitation-δD in China. The temperature data in plot *a* are derived from http://www.iaea.org/water. The temperature data in plots *b*–*g* are derived from the output data of the models corresponding to precipitation-δD

was higher than that in winter. The spatial pattern of δD in China is well modeled by the SWING2 models. However, there are deviations among these models (CAM, ECHAM, GISS_E, isoGSM, LMDZ, LMDZfree, and MIROC) controlled by factors such as the local topography, regional climate, and the scale of the study area. In addition, the numbers of samples and their position also influence the deviation. Wang et al. (2015) assessed the simulations from the SWING2 models (including ECHAM, LMDZ, LMDZfree, MIROC, and isoGSM) in the arid regions of central Asia and noted that the simulation in ECHAM was closest to the observation. In this paper, the simulated precipitation-δD in LMDZ is closest to the observation (GNIP and CHNIP) in terms of the correlation coefficient (Fig. 3). Unfortunately, LMDZ did not capture the low value of the meridional gradient around the Tibetan Plateau and its eastern region (e.g., Kunming, Lhasa and Ailaoshan shown in Fig. 4c). However, the CAM, GISS_E, and MIROC models capture the low value. With respect to the altitude effect, continental effect, and precipitation amount, the different models show different performance in illustrating the spatial pattern of the influencing factors in China. Therefore, it is difficult to select a best model among the SWING2 models for the entire region of China because there are extremely cold regions in the Tibetan Plateau and arid deserts in northwestern China. Moreover, it is very complicated to select a model for the monsoon and non-monsoon regions in China because of the water sources. It is necessary for us to choose an isotopic model in SWING2 following the purpose of the research and region of interest.

Conclusions

Most of the SWING2 models perform well with respect to the spatial pattern of the stable water isotope of the precipitation in China. The spatial patterns of δD of the precipitation derived from the models exhibit the same distribution compared with that from the measured data in GNIP and CHNIP. The high value center of the modeled δD appears in the southeastern region and

the Tarim Basin, and the low value is simulated in the Tibetan Plateau and northwestern and northeastern China. With respect to the correlation between observations and simulation, it seems that LMDZ performs best, with a high correlation coefficient (CC) of 0.78 and 0.57 corresponding to GNIP and CHNIP, respectively. The root mean square (RMS) is relatively low; however, there are relatively larger differences between the observation and LMDZ (Fig. 3). In addition, the LMDZ nudged by reanalysis is notably better than the free simulation (LMDZfree) in terms of RMS (Fig. 3b). With respect to the meridional gradient, the low values are captured by CAM, GISS_E, and MIROC (Fig. 4). The CAM and GISS_E are good at interpreting the altitude effect, while GISS_E and LMDZfree perform better in describing the continental effect for precipitation-δD in China. To illustrate the temperature and precipitation amount effects, the different models should be cautiously chosen for the interpretation of the specific issue in different regions, especially in the northwestern portion of China, although all of the models show a clear advantage.

The high-value regions of the simulated precipitation-*d* mainly occur in the Tibetan Plateau and the southern portion of eastern China, which is in agreement with the observation. The latitudinal gradient of *d* was successfully simulated using all SWING2 models. The results show a decreasing trend of *d* of the precipitation from west to east in China, and the difference among the models in the western region is larger than that in the eastern region. However, the results for the meridional gradient from the simulation are not significant. The change of the isotopes of precipitation for monthly variation has the strong temperature effect revealed by the models. However, it is notable that some models in SWING2 underestimate the value of δD of the precipitation compared with GNIP on a monthly scale, such as CAM, GISS_E, and MIROC, but isoGSM overestimates δD from May to October. In general, the simulations of LMDZ and LMDZfree are closest to the GNIP. Although most models overestimate *d* of the precipitation, the variation of all models is consistent with the GNIP.

Acknowledgments This work was supported by the National Natural Science Foundation of China (no. 41161012 and no. 41461003) and the National Basic Research Program of China (no. 2013CBA01801). The authors thank Stable Water Isotope Intercomparison Group, Phase 2 (SWING2) for providing the data (http://www.giss.nasa.gov/projects/swing2).

References

AGU (1995) U.S. National report to IUGG 1991–1994: contributions in atmospheric sciences. Boulder, Colorado, 7.

Araguás-Araguás L, Froehlich K, Rozanski K (2000) Deuterium and oxygen-18 isotope composition of precipitation and atmospheric moisture. Hydrol Process, 14(8): 1341–1355. doi:10.1002/1099-1085(20000615)

Cai Z, Tian L (2016) Atmospheric controls on seasonal and interannual variations in the precipitation isotope in the east Asian monsoon region. J Climate 29(4):1339–1352

Conroy JL, Cobb KM, Noone D (2013) Comparison of precipitation isotope variability across the tropical Pacific in observation and SWING2 model simulations. J Geophys Res Atmos 118(11): 5867–5892

Dansgaard W (1964) Stable isotopes in precipitation. Tellus B 16:436–468

Dincer T (1968) The use of oxygen 18 and deuterium concentration in the water balance of lakes. Water Resour Res 4(6):1289–1305

Gat JR, Mazor E, Tzur Y (1969) The stable isotope composition of mineral waters in the Jordan Rift Valley, Israel. J Hydrol 7(3):334–352

Gryazin V, Risi C, Jouzel J, Kurita N, Worden J, Frankenberg C, Bastrikov V, Gribanov K, Stukova O (2014) To what extent could water isotopic measurements help us understand model biases in the water cycle over western Siberia. Atmos Chem Phys 14(18): 9807-9830

Gu W (2011) Isotope hydrology. Science Press, Beijing

Haese B, Werner M, Lohmann G (2013) Stable water isotopes in the coupled atmosphere-land surface model ECHAM5-JSBACH. Geosci Model Dev 6:1463–1480

Hoffmann G, Werner M, Heimann M (1998) Water isotope module of the ECHAM atmospheric general circulation model: a study on timescales from days to several years. J Geophys Res Atmos 103(D14): 16871–16896

Kurita N, Noone D, Risi C, Schmidt GA, Yamada H, Yoneyama K (2011) Intraseasonal isotopic variation associated with the Madden-Julian oscillation. J Geophys Res Atmos 116(D24):D24101. doi: 10.1029/2010JD015209

Lee J-E, Fung I, DePaolo DJ, Henning CC (2007) Analysis of the global distribution of water isotopes using the NCAR atmospheric general circulation model. J Geophys Res Atmos 112(D16). doi:10.1029/2006JD007657

Li J, Pang Z, Kong Y, Huang TM, Zhou MZ (2014) Contrasting seasonal distribution of stable isotopes and deuterium excess in precipitation over China. Fresen Environ Bull 23(9): 2078-2085.

Liu J, Song X, Yuan G, Sun X, Yang L (2014) Stable isotopic compositions of precipitation in China. Tellus B 66:22567. doi:10.3402/tellusb.v66.22567

Pfahl S, Sodemann H (2014) What controls deuterium excess in global precipitation? Clim Past 10(2):771–781

Risi C, Bony S, Vimeux F, Jouzel J (2010) Water-stable isotopes in the LMDZ4 general circulation model: model evaluation for present-day and past climates and applications to climatic interpretations of tropical isotopic records. J Geophys Res Atmos 115(D12): D12118. doi:10.1029/2009JD013255

Risi C, Noone D, Worden J, Frankenberg C, Stiller G, Kiefer M, Funke B, Walker K, Bernath P, Schneider M, Bony S, Lee J, Brown D, Sturm C (2012a) Process—evaluation of tropospheric humidity simulated by general circulation models using water vapor isotopic observations: 2. Using isotopic diagnostics to understand the mid and upper tropospheric moist bias in the tropics and subtropics. J Geophys Res Atmos 117(D5):D05304. doi:10.1029/2011JD016623

Risi C, Noone D, Worden J, Frankenberg C, Stiller G, Kiefer M, Funke B, Walker K, Bernath P, Schneider M, Wunch D, Vanessa S, Deutscher N, Griffith D, Wennberg P, Strong K, Smale D, Mahieu E, Barthlott S, Hase F, García O, Notholt J, Warneke T, Toon G, Sayres D, Bony S, Lee J, Brown D, Uemura R, Sturm C (2012b) Process—evaluation of tropospheric humidity simulated by general circulation models using water vapor isotopologues: 1. Comparison between models and observations. J Geophys Res Atmos 117(D5): D05303. doi:10.1029/2011JD016621

Schmidt GA, LeGrande AN, Hoffmann G (2007) Water isotope expressions of intrinsic and forced variability in a coupled ocean-atmosphere model. J Geophys Res Atmos 112(D10):D10103. doi:10.1029/2006JD007781

Schotterer U, Oldfield F, Fröhlich K (1996) Global network for isotopes in precipitation. Bern, Switzerland, pp. 15–26

Song X, Liu J, Sun X, Yuan G, Liu X, Wang S, Hou S (2007) Establishment of Chinese network of isotopes in precipitation (CHNIP) based on CERN. Adv Earth Sci 22(7):738–747

Sturm C, Zhang Q, Noone D (2010) An introduction to stable water isotopes in climate models: benefits of forward proxy modeling for paleoclimatology. Clim Past 6(1):115–129

Taylor KE (2001) Summarizing multiple aspects of model performance in a single diagram. J Geophys Res 106(D7):7183–7192

Tian L, Yao T, MacClune K, White JWC, Schilla A, Vaughn B, Ichiyanagi K (2007) Stable isotopic variations in West China: a consideration of moisture sources. J Geophys Res Atmos 112(D10):D10112. doi:10.1029/2006JD007718

Tindall JC, Valdes PJ, Sime LC (2009) Stable water isotopes in HadCM3: isotopic signature of el Nino southern oscillation and the tropical amount effect. J Geophys Res Atmos 114(D4):D04111. doi:10.1029/2008JD010825

Wang S, Zhang M, Chen F, Che Y, Du M, Liu Y (2015) Comparison of GCM-simulated isotopic compositions of precipitation in arid Central Asia. J Geogr Sci 25(7):771–783

Worden J, Noone D, Bowman K, Beer R, Eldering A, Fisher B, Worden H (2007) Importance of rain evaporation and continental convection in the tropical water cycle. Nature 445(7127):528–532

Xi X (2014) A review of water isotopes in Atmospheric General Circulation Models: Recent advances and future prospects. International Journal of Atmospheric Sciences 2014. doi: 10.1155/2014/250920

Yoshimura K, Kanamitsu M, Noone D, Oki T (2008) Historical isotope simulation using reanalysis atmospheric data. J Geophys Res Atmos 113(D19):D19108. doi:10.1029/2008JD010074

Zhang M, Wang S (2016) A review of precipitation isotope studies in China: basic pattern and hydrological process. J Geogr Sci 26(7):921–938

Zhang X, Liu J, Tian L, Yao T (2004) Variations of $\delta^{18}O$ in precipitation along vapor transport paths over Asia. Acta Geogr Sinica 59(5):699–708

Zhang X, Sun Z, Guan H, Zhang X, Wu H, Huang Y (2011) GCM simulation of stable water isotopes in water cycle and intercomparisons over East Asia. J Glaciol Geocryol 33(6):1274–1285

Zhang X, Sun Z, Guan H, Zhang X, Wu H, Huang Y (2012) GCM simulation of stable isotopes in the water cycle in comparison with GNIP observation over East Asia. Acta Meteorol Sin 26: 420-437.